Conference Paper, Published Version

Paul, Thomas; Lutringer, Clément; Poupardin, Adrien; Bennabi, Abdelkrim; Jeong, Jena; Sergent, Philippe

Wave overtopping and overflow hazards: application on the Camargue sea-dike

Zur Verfügung gestellt in Kooperation mit/Provided in Cooperation with:
TELEMAC-MASCARET Core Group

Wave overtopping and overflow hazards: application on the Camargue sea-dike

Thomas Paul, Clément Lutringer, Adrien Poupardin,
Abdelkrim Bennabi, Jena Jeong

Institut de Recherche en Constructibilité, Ecole Spéciale des Travaux Publics
Université Gustave Eiffel
6-8 avenue Blaise-Pascal Cité Descartes – Champs-sur-Marne – 77455 Marne La Vallée, France.
apoupardin@estp-paris.eu

Philippe Sergent
CEREMA EMF
134 rue de Beauvais, CS 60039, 60280 Margny les Compiègne Cedex, France
Philippe.Sergent@cerema.fr

Abstract— **Dike breaches occurs regularly during storm events. This phenomenon contributes to amplify considerably the impact of floods on coastal areas. It represents an important cost for repairing existing infrastructures in the vicinity of the sea-dike. Then, they must be upgraded to prevent breaches.**

In the present study, ANEMOC and REFMAR dataset were analysed, off Camargue coasts, to quantify the storm hazards in terms of wave height and sea level wind set-up. Repartition laws were adjusted on dataset to build a 2D-copula which is used to estimate events return periods.

As we were interested in the physical parameters around the sea-dike, waves were propagated from the deep water by using TOMAWAC module which takes into account the actual bathymetry. As a first approximation, only a 1D propagation was considered.

From estimated local parameters, overtopping formula were used to estimate the overtopping discharge, the crest velocity, and the water level over the sea-dike. These latter were used to assess a potential erosion on the dike rear-side.

A set of several wave heights – sea-level wind set-up couple were tested and each of them were relied to a probability of occurrence given by the 2D-copule.

I.   INTRODUCTION

Hazards studies are of a great importance to size infrastructures which protect a city or a socio-economic area. In particular, in the case of coastal storms, we consider wave spectra and their propagation to coasts, mean water level and dike dimensions which impact flood probability of occurrence.

Previous works in storm hazards ([1] and [2]) allow to estimate the wave height and water level return periods, in particular, concerning extreme events.

Depending of these deep water parameters, waves can be propagated using empirical formula [3] or tools based on wave spectrum propagation by considering the dispersion relation, in particular in intermediate water depths (TOMAWAC module for example [11]). The wave breaking impacts greatly the propagation by decreasing linearly wave heights and increasing the wave set-up to the coast with a maximum at toe of sea-dike.

From local parameters, coupled software can be used to compute water discharges over the dike (by using the TELEMAC suit for example). Water discharge estimation can also be deduced from empirical laws ([4], [5] and [6] for example).

In the scope of this study, several approaches were combined and compared to estimate the water discharge over the sea-dike and his corresponding water crest velocity which may be responsible for dike rear-side erosion.

In Part II, input parameters and numerical model are presented. Part III is focused on numerical results and their interpretations. Part IV deals with water discharges and particularly run-off velocities. Finally, we conclude this study in Part V.

II.   INPUT PARAMETERS AND NUMERICAL MODEL

A.   Probabilistic data

For this study, two sets of data were considered: REFMAR data extracted from the tide gauge located in Marseille harbour and ANEMOC data from a synthetic wave gauge located at a depth of 30 m and 3.6 km off the coast. Event were selected by identifying a local maximum and by considering a minimum time interval of 24 h between two events.

Both datasets were analysed to extract storm events by considering a two-thresholds method. Then, we use a Generalized Extreme Value Distribution (GEV) to fit REFMAR and ANEMOC treated data independently [7].

Finally, a Gumbel Copula, called F in the following of the text, was used to merge both distributions by sector and we determined the interdependency parameter α by using a likelihood maximum method.

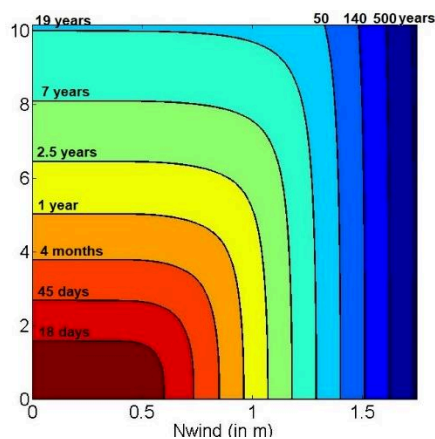The computed Gumbel Copula is given in Figure. 1.

Figure. 1. Gumbel copula built from ANEMOC and REFMAR dataset and by fitting events with a Generalized Extreme Value Distribution (GEV)

B. Physical input Parameters

TOMAWAC module [8], from TELEMAC software suite, was used to propagate the wave from deep waters to the coast.

Bathymetry was built from Litto3D products (see www.shom.fr for more details) for shallow water ($d < 10$ m) and GEBCO (see www.gebco.net for more details) data for deeper water. A representation of the two-dimensional bathymetric map is given in Figure. 2.
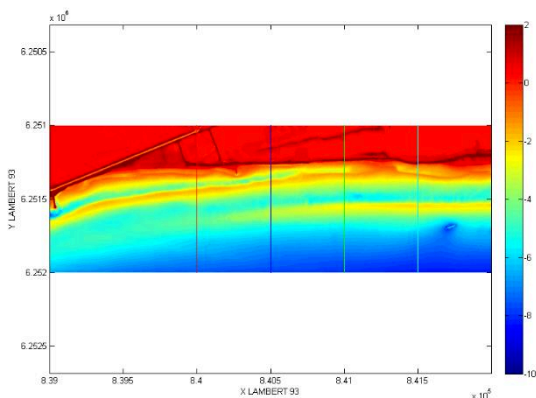

Figure. 2. Bathymetric map in Lambert 93 coordinates system from Litto3D products

As a preliminary work, we consider a one-dimensional wave propagation from the south (deep water) to the north on the profile $X = 841000$ (in green in Figure 2) in Lambert 93 coordinates system (see Figure 3) although three event classes were detected (REFMAR data) and separated according to their propagation direction: north-west (315° for most energetic and frequent extreme events), north (0°) and east (80°). Then, we neglected refraction effects in the scope of this paper.

Concerning other physical parameters, simulations were realized by varying: significant wave height H_{m0} from 2 to 10 m each 2 m and; mean water level $\overline{\eta_{wind}}$ from 0 to 2 m each 0.5 m.
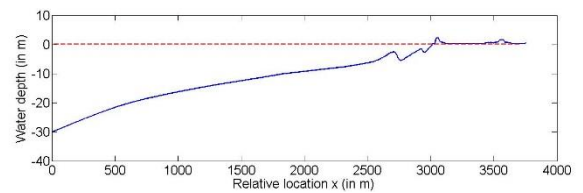

Figure. 3. Bathymetric profile $X = 841000$ in Lambert 93 coordinates system. Water depth was replaced in a relative coordinate system with x designing the propagation direction and the new reference $x = 0$ corresponding to $Y = 6254300$ in Lambert 93 coordinates system. Waves propagates from the south to the north.

C. Numerical input Parameters

We chose to propagate a JONSWAP spectrum in the TOMAWAC options by adjusting the significant wave height and pic frequency to simulate the case described section II-B. To simplify the problem, ANEMOC data were used to fit relation (1) which rely the significant wave height to the wave peak period.

$$\frac{1}{f_p} = 3.72 \, H_{m0}{}^{0.37} \tag{1}$$

We verified that (1) is not so far from the constant curvature hypothesis in deep water. Furthermore, the exponent in (1) is slightly inferior to the one given in the literature, as in [9].

The frequency sampling was adjusted from $f = 0.05$ Hz (20 s) to $f = 0.5$ Hz (2 s) with a frequency ratio of 1.1.

The spatial grid was sampled by using a spatial step of 3 m (in x and y-directions). We considered a flume width of 60 m.

The total time was fixed to ensure that a permanent state is reached in TOMAWAC at the simulation end. The time step of simulation was fixed to 0.5 s.

Battjes and Janssen's model (1978) was used to take into account the wave breaking in the simulation, and we chose the Miche's criterion to rely the local wave height to the water depth by using typical values for α, γ_1 and γ_2.

D. Laws for wave overtopping

Finally, TOMAWAC results (local wave height H_m and mean water level $\overline{\eta_t} = \overline{\eta_{wind}} + \overline{\eta_{wave}}$) were extracted at toe of dike at a water depth of $d = 0.5$ m (see Figure 4).

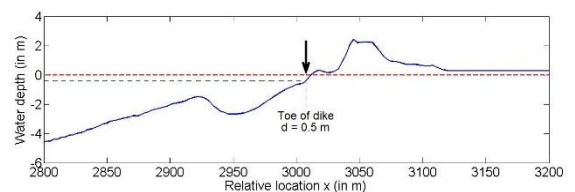Figure 4. Bathymetric profile: zoom on the dike

The wave set-up $\overline{\eta_{wave}}$ was computed at each point from the deep water by using the radiative stress Sxx gradient.

As shown in Figure 4, the upstream bank of the dike is located near an emerged reef flat which must be taken into account when applying overtopping formula. In this paper, the form developed by [10] was considered:

$$\frac{q_w}{\sqrt{g\,Hm^3}} = 0.06 \frac{\xi_{op}}{\sqrt{\tan(\alpha)}} \exp\left(-5.2 \frac{R_c}{Hm} \frac{1}{\xi_{op}} \frac{1}{\gamma_r\gamma_b\gamma_h\gamma_\beta}\right) \text{for } \xi_{op} < 2 \quad (2)$$

$$\frac{q_w}{\sqrt{g\,Hm^3}} = 0.2 \exp\left(-2.6 \frac{R_c}{Hm} \frac{1}{\gamma_r\gamma_b\gamma_h\gamma_\beta}\right) \text{for } \xi_{op} > 2 \quad (3)$$

with q_w the overtopping discharge, α the slope of the dike front-side, R_c (vertical distance between the still water elevation and crest elevation) the freeboard, ξ_{op} the Iribarren number and γ-factors reduction factors (see [5]). For applying these formulas, we measured $\alpha = 26°$, ξ_{op} depended on the simulated case, $\gamma_r = 0.6$ (for one natural blocks layer) and γ_b depending on the local water level and on the reef flat elevation and length (see [4]).

These estimated values were compared with discharge computed with results given by using Dean formula (4) and Henderson law (5) [11]:

$$\overline{\eta_t} = \overline{\eta_{dean}} = \overline{\eta_{wind}} + 0.191 H_{m0} \quad (4)$$

$$q_w = 0.5443 \sqrt{g\,h_0{}^3} \quad (5)$$

with h_0 corresponding to the vertical distance between the still water elevation $\overline{\eta_{dean}}$ and crest elevation.

The two methods will be referred as Met. a) (TOMAWAC for wave propagation and (2) or (3) for discharge estimation) and as Met. b) ((4) for water level and (5) for discharge estimations). A diagram describing both methods is given Figure 5.
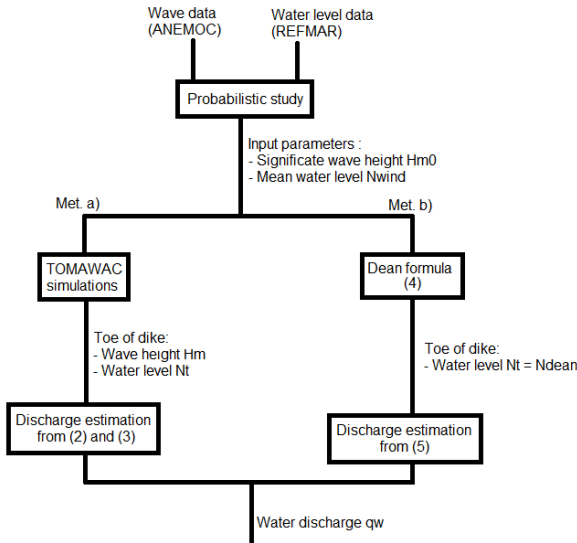

Figure 5. Methodology for water discharge estimation

Finally, TELEMAC-2D (Shallow-Water equations) was used to submerge the dike in two cases: moderate and severe flooding and to compare results with Met. a) and b). For these simulations, we considered results of TOMAWAC simulations as input parameters. To simplify the problem, we considered a monochromatic wave signal with wave height equal to the corresponding significate wave height computed with TOMAWAC and water level impacted by the wave set-up. The bathymetric grid input boundary is located at toe of dike (see Figure 4). We measured wave discharges, water heights and

velocities by using synthetic gauges located on the dike crest and the dike rear-side.

III. RESULTS

A. TOMAWAC results

Each case was simulated by using TOMAWAC module. Significant wave heights H_m and mean water level $\overline{\eta_t}$, at toe of dike ($d = 0.5$ m), are shown in Figure 6.
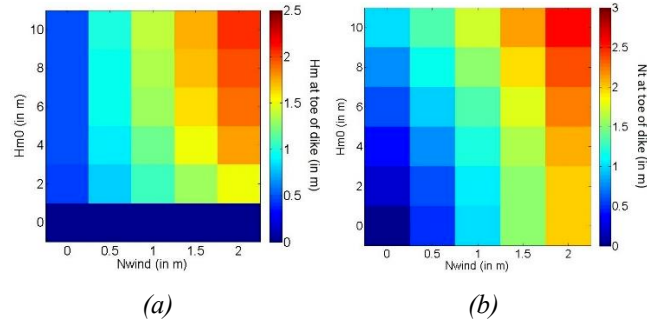

(a) *(b)*

Figure 6. Hydraulics parameters at a water depth $d = 0.5\,m$ at toe of dike: (a) significate wave height $Hm(d = 0.5$ m); (b) mean water level $\overline{\eta_t}(d = 0.5$ m)

By considering a crest elevation of 2.31 m, overtopped discharges were computed by using Met. a) and Met. b). Data were oversampled on a slightly more resolved grid (see Figure 7a) and b)). We remind that the horizontal distance between toe of dike and crest elevation is around 33 m.

Generally, Met. a) (Figure 7a) induces higher discharge for higher wind set-up and lower significant wave height whereas Met. b) (Figure 7b) induced higher discharge for lower wind set-up and higher significant wave heights.
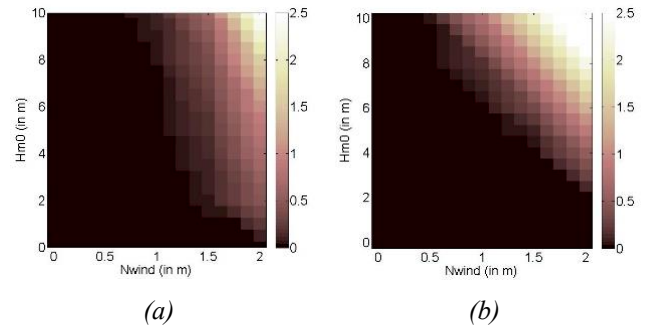

(a) *(b)*

Figure 7. Overtopping discharge in $[m^3/s/m]$ computed from: (a) Met. a); (b) Met. b)

As expected, Met. b) (Figure 7b) give linear iso-discharge lines whereas Met. b) (Figure 7a) shows curbed iso-discharge lines.

B. Discharge occurrences on the dike

By combining the Gumbel copula shown in Figure 1 and discharge grids obtained in Figuire 7, each event can be associated to an overtopping discharge and a return period. For example, a 5 m significant wave height and 1 m wind set-up event corresponds to a 2.5 years return period event but it doesn't generate high discharge over the dike (0.011 and 0

$m^3/s/m$ with Met. a) and Met. b) respectively). Whereas a 6 m significant wave height and 1.5 m wind set-up event corresponds to a 130 years return period and it generates high flooding: 0.2 and 0.33 $m^3/s/m$ with Met. a) and Met. b) respectively.

Then, we wanted to know what is the cumulative probability to reach: a moderate discharge (0.01 $m^3/s/m$), a severe discharge (0.2 $m^3/s/m$). Cumulative probabilities of Gumbel copula were integrated on the two latter iso-discharge lines for Met. a) and b).

Knowing what couple $(\overline{\eta_{wind}}, H_{m0})$ of variables would give us a specified discharge, we then had to integrate the copula represented in Figure1 on all the points that would give us this amount of discharge (or worse). We decide to integrate the derivative of the copula $\frac{\partial F(\overline{\eta_{wind}}, H_{m0})}{\partial H}$ on the iso-discharge line, which should be the same according to theory.

$$P(\eta > \bar{\eta}_t) = \iint_C \left(\frac{\partial^2 F(\overline{\eta_{wind}}, H_{m0})}{\partial H \partial \eta} \right) d\eta dH \qquad (6)$$

$$P(\eta > \bar{\eta}_t) = \int_0^{+\infty} \left[\frac{\partial F(\overline{\eta_{wind}}, H_{m0})}{\partial H} \right]_{g(H)}^{+\infty} dH \qquad (7)$$

$$P(\eta > \bar{\eta}_t) = -\int_0^{+\infty} \left(\frac{\partial F(\overline{\eta_{wind}}, H_{m0})}{\partial H} (H, g(H)) \right) dH \qquad (8)$$

with $P(\eta > \bar{\eta}_t)$ the exceedance probability over a water level $\bar{\eta}_t$ and $g(H)$ the law relying η and H which can be easily deduced from data of Figure 7a and 7b (we assume that iso-discharge lines can be converted into iso-water level lines).

Components of the copula derivative $\frac{\partial F(\overline{\eta_{wind}}, H_{m0})}{\partial H}$ were summed onto the line $\bar{\eta}_t = g(H)$ for Met. a) and Met. b) by varying the discharge (0.01 and 0.2 $m^3/s/m$). Results are shown in Figure 8.
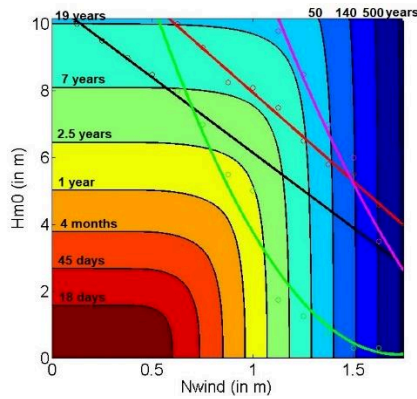

Figure 8. Gumbel copula in logarithmic scale and iso-discharge lines for: a discharge exceedance of 0.01 $m^3/s/m$ by using Met. a) (in green) and Met. b) (in black); a discharge exceedance of 0.2 $m^3/s/m$ by using Met. a) (in magenta) and Met. b) (in red)

The return period (computed from (8)) for discharge exceedances of 0.01 and 0.2 $m^3/s/m$ are respectively of 1 year (Met. a)), 2 years (Met. b)) and 75 years (Met. a)), 7 years (Met. b)). As Met. b) is supposed to be used as a first estimation, the return period of a 0.2 $m^3/s/m$ water discharge must be closer to probability of occurrence given by Met. a).

C. *Comparison with TELEMAC-2D simulations*

For TELEMAC-2D, cases described as moderate (0.011 $m^3/s/m$) and severe (0.2 $m^3/s/m$) in section III-B were simulated.

In the scope of this paper, we focused our analysis on the first wave which overtopped the dike.

Figure 9 shows differences between both cases. In particular, the severe event gives a maximum water discharge of 2.5 $m^3/s/m$ followed by a positive discharge during the whole wave period (7.2 s for a wave height of 6 m). Whereas the moderate event gives a smaller peak discharge of 0.03 $m^3/s/m$ with a water discharge more regular in time.

By integrating these water discharges on a period, we retrieved a mean water discharge of 0.012 $m^3/s/m$ (closed from results of Met. a)) for the moderate event and of 0.322 $m^3/s/m$ (closed from results of Met. b)) for the severe event.
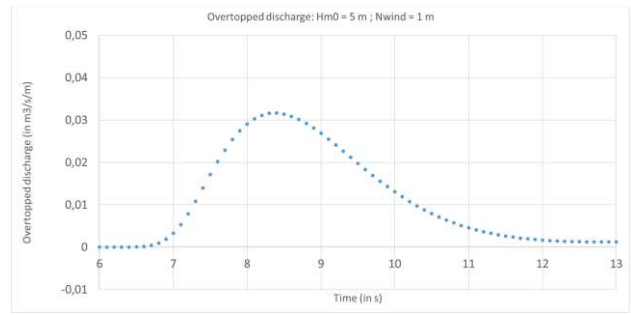
(a)
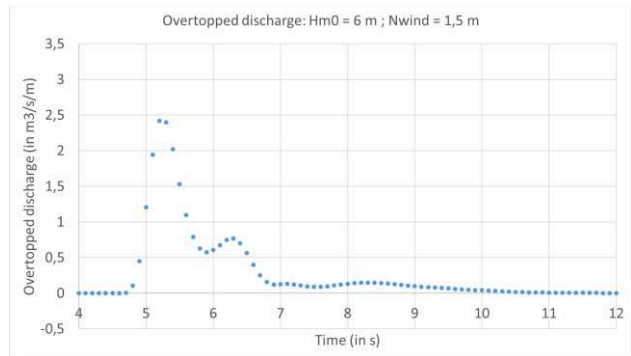
(b)

Figure 9. Overtopping discharge in [$m^3/s/m$] computed with TELEMAC-2D by considering the following simulated cases: (a) a 5 m significant wave height and 1 m wind set-up event; (b) a 6 m significant wave height and 1.5 m wind set-up event

IV. DISCUSSION

A. In terms of peak velocity

As, we are interested in the dike rear-side erosion, we used the relation (9) given by [6] to convert the water volume V into a peak velocity u_p:

$$u_p = 4.5 V^{0.3} \qquad (9)$$

The volume depends on the considered point onto the iso-discharge lines $\overline{\eta_t} = g(H)$. Indeed, the discharge is linked to the wave period which is linked to the significate wave height. Then, by considering parameters described in section III-B and eq. (9), mean water discharges of 0.01 and 0.2 $m^3/s/m$ correspond to peak velocities of 2.1 and 5 m/s.

By using results from TELEMAC-2D, peak velocities of 0.7 m/s and 2.6 m/s respectively were obtained on the dike rear-side.

Orders of magnitude seem to be respected but results from TELEMAC-2D present the advantage to take into account for the actual topography.

Depending on the soil characteristics, these peak velocities, corresponding to return periods of 100 and 1000 years, should generate erosion as we observed periodically breaches onto the Camargue sea-dike.

V. CONCLUSION AND PERSPECTIVES

Wave parameters (local water level $\overline{\eta_t}$ and wave height H_m) were estimated at toe of dike for several initial parameters couples ($\overline{\eta_{wind}}, H_{m0}$) and their corresponding return periods.

Two methods were proposed to estimate the water discharge over the sea-dike and we found distributions of water discharges depending on initial parameters couples. We used it to compute cumulative probabilities associated to moderate (0.01 $m^3/s/m$) and severe (2 $m^3/s/m$) events. Return periods around 1.5 and 75 years respectively were found.

As, we were interested in the dike stability, water peak velocities on the dike rear-side were also estimated. For these kind of events, we retrieved that erosion may occur depending on the critical velocity of the dike soil composition.

In perspectives of this work, the use of TOMAWAC in two dimensions is expected to take into account effects of refraction and we will compare our results with the approach developed by [3].

Finally, for future works on Camargue sea-dike rear-side erosion, we will, particularly, pay attention to the peak water discharge which may be responsible for the erosion process beginning.

It remained important to improve our results precision to adapt the dike against extreme events.

REFERENCES

[1] Salvatori, G., 2004. Bivariate return periods via 2-Copulas, Statistical Methodology, vol. 1, pp. 129-144.

[2] Brunner, M. I., Favre, A.-C., Seibert, J., 2016. Bivariate return periods and their importance for flood peak and volume estimation, WIREs Water, 3(6), pp. 819-833.

[3] Goda, Y., 1970. Numerical experiments on wave statistics with spectral simulation, Rep. Portand Harbour Res. Inst.

[4] EurOtop, 2018. Manual on wave overtopping of sea defences and related structures, Van der Meer, J.W., Allsop, N.W.H., Bruce, T., De Rouck, J., Kortenhaus, A., Pullen, T., Schüttrumpf, H., Troch, P. and Zanuttigh, B., www.overtopping-manual.com.

[5] Hughes, S.A., Nadal, N.C., 2009. Laboratory study of combined wave overtopping and storm surge overflow of a levee, Coastal Engineering 56, pp. 244–259.

[6] Van der Meer, J., van Hoven, A., Paulissen, A., Steendam, G., Verheij, H., Hoffmans, G., Kruse, G., 2012. Handreiking toetsen grasbekledingen op dijken t.b.v het opstellen van het beheerdersoordeel (bo) in de verlengde derde toetsronde. Tech. rep., Rifkswatershaat, Ministerie van Infrastructuur en Milieu.

[7] Muraleedharan, G., Guedes Soares, C., Lucas C., 2010. Characteristic and Moment Generating Functions of Generalised Extreme Value Distribution (GEV), Sea Level Rise, Coastal Eng., Shorelines and Tides, Chapter 13, Publisher: Nova Science Publishers, New York.

[8] Fouquet, T., 2016. Telemac Modeling System, Tomawac Software, Release 7.1, operating manual,

[9] Goda, Y. 2000. Random seas and design of maritime structures (2nd edition). World Scientific, Singapore, ISBN 981-02-3256-X.

[10] van der Meer, J.W., Janssen, W., 1995. Wave run-up and wave overtopping at dikes; In: Kabayashi, Demirbilek (Eds.), Wave Forces on Inclined and Vertical Wall Structures; American Society of Civil Engineers, pp. 1–27.

[11] Henderson, F.M., 1966. Open channel flow. MacMillian Publishing Co., New York